Inorganic Chemistry

Article

pubs.acs.org/IC

Photodriven Oxygen Removal via Chromophore-Mediated Singlet Oxygen Sensitization and Chemical Capture

Ryan M. O'Donnell,*[,†] Tod A. Grusenmeyer,*[,‡] David J. Stewart,[‡,§] Trenton R. Ensley,[†] William M. Shensky, III,[†] Joy E. Haley,[‡] and Jianmin Shi[†]

[†]U.S. Army Research Laboratory, 2800 Powder Mill Road, Adelphi, Maryland 20783-1138, United States

[‡]Air Force Research Laboratory, Wright Patterson Air Force Base, Ohio 45433-7750, United States

[§]General Dynamics Information Technology, 5100 Springfield Pike, Dayton, Ohio 45431, United States

Supporting Information

ABSTRACT: We report a general, photochemical method for the rapid deoxygenation of organic solvents and aqueous solutions via visible light excitation of transition metal chromophores (TMCs) in the presence of singlet oxygen scavenging substrates. Either 2,5-dimethylfuran or an amino acid (histidine or tryptophan methyl ester) was used as the substrate in conjunction with an iridium or ruthenium TMC in toluene, acetonitrile, or water. This behavior is described for solutions with chromophore concentrations that are pertinent for both luminescence and transient absorption spectroscopies. These results consistently produce TMC lifetimes comparable to those measured using traditional inert gas sparging and freeze–pump–thaw techniques. This method has the added benefits of providing long-term stability (days to months); economical preparation due to use of inexpensive, commercially available oxygen scrubbing substrates; and negligible size and weight footprints compared to traditional methods. Furthermore, attainment of dissolved $[O_2] < 50\ \mu M$ makes this method relevant to any solution application requiring low dissolved oxygen concentration in solution, provided that the oxygenated substrate does not interfere with the intended chemical process.

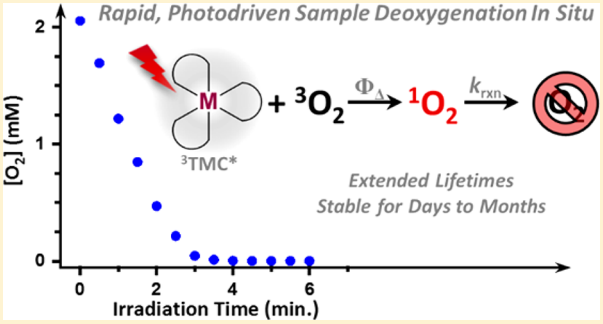

INTRODUCTION

Widespread interest in transition metal chromophores (TMCs) continues to grow as they are applied in photocatalysis,[1,2] biological sensing,[3,4] dye-sensitized solar cells (DSSCs),[5−7] photodynamic therapy (PDT),[8] and nonlinear optical (NLO) applications.[9,10] Their popularity arises from their synthetic and redox tunability and photophysical properties. TMCs that possess metal-to-ligand charge transfer (MLCT) excited states are of particular interest due to excited state lifetimes on the order of hundreds of nanoseconds to tens of microseconds and moderate to high photoluminescence quantum yields.[11]

Characterization of long-lived, luminescent chromophores is complicated by oxygen dissolved in organic solvents (1−5 mM) and water (0.3 mM) due to the efficient, collisional quenching of molecular excited states by ground state oxygen.[12] In this process, ground state oxygen, which possesses a triplet spin multiplicity, $^3O_2$, is promoted to an excited state of singlet spin multiplicity, $^1O_2$ ($^1\Delta_g$), while returning the excited chromophore to its ground state, eqs 1−3.[13,14] Many TMCs possess large quantum yields for $^1O_2$ production, $\Phi_\Delta = 0.5-1$.[15,16] Excited state quenching decreases the observed lifetime, τ_{obs}, and the luminescence quantum yield of the chromophore; thus, care is often taken to deoxygenate samples either through inert gas sparging (N_2 or Ar) or through the freeze–pump–thaw degas method.

Although this quenching process is detrimental to long lifetime and luminescence applications, the $^1O_2$ produced can be advantageous for synthetic or photobiological applications when it reacts with substrates dissolved in solution. For instance, unity Φ_Δ values are advantageous for PDT applications where directed irradiation generates $^1O_2$ which attacks tumor cells.[8,14] In terms of organic photochemistry, the Schenck ene reaction is an important pathway for the addition of oxygen atoms across carbon–carbon double bonds.[17] Interestingly, this seemingly antagonistic pairing of excited state quenching and $^1O_2$ production provides for an alternative method of oxygen removal from solution. A substrate known to react irreversibly with $^1O_2$ is added to an aerated solution of a given chromophore. Upon irradiation, oxygen is permanently abstracted from solution as the photogenerated $^1O_2$ reacts with the scavenging substrate. Recent literature reports demonstrated the applicability of sodium sulfite as a photochemical oxygen scavenger in aqueous solution and oleic acid, 9,10-dimethylanthracene, and 2,5-dimethylfuran as photochemical oxygen scrubbers in liquid polyethylene glycol.[18,19] Consequently, an expansion of these results to encompass a comprehensive methodology for the

Received: May 26, 2017
Published: July 11, 2017

DOI: 10.1021/acs.inorgchem.7b01226
Inorg. Chem. 2017, 56, 9273−9280

photochemical deoxygenation of polar, nonpolar, and aqueous solutions is necessary and would be valuable.

Our general, photochemical approach focused on the deoxygenation of toluene, acetonitrile, and water solutions containing TMCs and either 2,5-dimethylfuran (organic solvents) or an amino acid (aqueous solutions of tryptophan and histidine). The oxygen removal substrates are inexpensive and available on the kilogram scale from major chemical suppliers (2,5-dimethylfuran ~ $1.00 per gram; histidine < $0.60 per gram; and L-tryptophan methyl ester ~ $5.00 per gram; see Supporting Information). The convenience and economical nature of this procedure make it applicable as an alternative deoxygenation method for photochemical systems when Ar or N_2 is not available or samples are required to remain deoxygenated for long time periods (e.g., days to months). Moreover, unlike large inert gas tanks and cumbersome vacuum pumps, there are no space requirements or maintenance costs associated with this method. This method could serve as a solution deoxygenation technique for any solution application requiring low dissolved oxygen concentrations as long as the oxygenated substrate does not interfere with the intended chemical process.

$$^1\text{TMC} \xrightarrow{h\nu} {}^1\text{TMC}^* \quad (1)$$

$$^1\text{TMC}^* \xrightarrow{k_{isc}} {}^3\text{TMC}^* \quad (2)$$

$$^3\text{TMC}^* \xrightarrow{^3O_2} {}^1\text{TMC} + {}^1O_2(^1\Delta_g) \quad (3)$$

$$\text{scavenger} \xrightarrow{^1O_2(^1\Delta_g)} [\text{scavenger-O}_2]\text{complex} \quad (4)$$

EXPERIMENTAL SECTION

General. Tris(2,2′-bipyridine)ruthenium(II) dichloride and all other reagents and solvents were purchased from Sigma-Aldrich and used as received. Tris(2,2′-bipyridine)ruthenium(II) dihexafluorophosphate was prepared from the anion metathesis reaction of tris(2,2′-bipyridine)ruthenium(II) dichloride with potassium hexafluorophosphate. ^{1}H NMR spectra were measured on a Bruker 600 MHz Avance NMR spectrometer, referenced to the internal residual solvent peak, and processed using TopSpin 3.5 software. Argon gas (Airgas, 99.999%) was used to sparge spectroscopic samples.

Synthesis of $[Ir^{III}(pbt)_2(dpm)]^0$. The compound was synthesized using previously reported procedures.[20,21] The free ligand 2,2′,6,6′-tetramethyl-3,5-heptanedione, dpm, (0.80 mL, 3.8 mmol) was added to a suspension of $[Ir(pbt)_2Cl]_2$ dimer (0.2501 g, 0.19 mmol) in dichloromethane. Tetrabutylammonium hydroxide (1.0 M in MeOH, 9.0 mmol) was added to the mixture which was subsequently refluxed for 16 h under nitrogen. After being cooled to room temperature, the crude reaction mixture was filtered through a silica plug using dichloromethane as the eluent. The solution volume was decreased under reduced pressure via rotary evaporator and ethanol was added to induce precipitation. The suspension was cooled in a refrigerator (3 °C) for 1 h to yield an orange microcrystalline powder. The precipitate was collected by vacuum filtration on a Buchner funnel, washed with cold ethanol, diethyl ether, and hexanes, and dried in a vacuum oven (55 °C) to recover 0.2394 g of orange powder (3.0 mmol, 78% yield). ^{1}H NMR ($(CD_3)_2CO$, 600 MHz): 8.16 (dd, 2H, J = 7.8, 0.6 Hz), 8.02 (d, 2H, J = 7.8 Hz), 7.75 (dd, 2H, J = 7.2, 0.6 Hz), 7.52 (td, 2H, J = 7.8, 1.2 Hz), 7.45 (td, 2H, J = 7.8, 1.2 Hz), 6.86 (td, 2H, J = 7.2, 1.2 Hz), 6.62 (td, 2H, J = 7.2, 1.8 Hz), 6.50 (d, 2H, J = 7.8 Hz), 5.49 (s, 1H), 0.82 (s, 18H).

UV−visible Absorption. UV−vis absorption spectra were recorded using a Shimadzu UV-2700 spectrophotometer for 2.0 mm borosilicate glass cuvettes (Spectrocell) or a Cary 5000 spectrophotometer for 1.0 cm cuvettes.

Irradiation Sources. The laser light output of a 30 mW 450 nm CW diode laser (World Star Tech, TECBL-30G-450) was passed through a 3.0 mm iris for excitation of 2 mm cuvette samples with an irradiance of 66 mW/cm^2. For 1.0 cm cuvette samples, excitation was performed using either a Quantel Vibrant Nd:YAG laser (5 ns fwhm, 10 Hz) equipped with an OPOTEK OPO tuned to 450 nm (6.6−8.8 mJ/cm^2 per pulse or a 450 W Xe arc lamp. The arc lamp light path proceeded through a 1/8 in. iris positioned 1.5 in. from the center of the cuvette. The diameter of the beam expanded to approximately 3/8 in. at the center of the cuvette.

Spectroscopy. Nanosecond transient absorption measurements on 2.0 mm cuvette samples were collected using a quasi-collinear pump−probe geometry, in which the pump and probe beams incident on the sample are separated by a small angle (<10°), in an Ultrafast Systems EOS transient absorption spectrometer. The 400 nm pump beam was generated by frequency doubling of the 800 nm pulse from a Spectra-Physics Solstice femtosecond amplifier system comprised of a Mai Tai Ti:sapphire oscillator and an Empower pump laser. The Solstice produced an average power of 3.5 W at 800 nm with a repetition rate of 1 kHz (100 fs fwhm pulse). The white-light continuum probe pulse was generated using a photonic crystal fiber (350−950 nm, 0.5 ns pulse width, 20 kHz repetition rate) that synchronized with the 400 nm pump beam. The pump−probe delay time was controlled by a digital delay generator with the probe light detected by a fiber-optic coupled multichannel spectrometer with a complementary metal-oxide-semiconductor (CMOS) sensor. For 1.0 cm cuvette samples, luminescence lifetimes were obtained using an Edinburgh Instruments LP920. Sample excitation was carried out using a Q-switched Nd:YAG laser (Quantel Vibrant, ca. 5 ns fwhm, 10 Hz repetition rate) equipped with an OPOTEK OPO tuned to 450 nm. Lifetimes were measured with a Hamamatsu R928 PMT and Tektronix TDS 3012C Digital Storage Oscilloscope. Electronic synchronization was controlled by Edinburgh Instruments F900 software. Laser excitation of the samples were aligned 90 deg relative to the white light probe beam which passed through the sample, then through a Czerny−Turner monochromator (300 mm focal length, 1800 grooves per mm grating, 500 nm blaze, < 2 nm bandwidth) before being passed to the PMT. To avoid excessive oxygen removal while collecting luminescence lifetimes, decay traces were the average of only three laser pulses.

Data Analysis and Fitting. All transient absorption data were corrected by subtracting spectral background features and applying t_0 corrections using Surface Explorer Pro 4.0 (Ultrafast Systems). Nanosecond transient absorption data analysis, fitting, and plotting were performed in OriginPro 2017. Least-squares error minimizations were accomplished using the Levenberg−Marquardt iteration method. Luminescence lifetime data were fit using the provided Edinburgh Instruments software. Subsequent kinetic irradiation data were plotted using OriginPro 9.1.

RESULTS AND DISCUSSION

Experiments to establish the viability of this photochemical deoxygenation methodology were performed in iterative fashion. Initial studies were carried out in 2 mm cuvettes and characterized using a nanosecond transient absorption (TA) geometry in which the pump and probe beams are separated by a small angle. This work was then expanded to include a thorough characterization of the chemical deoxygenation process in 1 cm cuvettes with TMC concentrations pertinent to both luminescence and TA spectroscopies.

The introductory set of 2 mm cuvette samples were prepared by dissolving the TMC of interest in the appropriate solvent in cuvettes equipped with stir bars. Care was taken to minimize the headspace in the cuvettes, and PTFE stoppers were used to seal the cells. We estimate that the oxygen content of a 5 μL air bubble present in the headspace of a cuvette would be less than 5% of the total amount of oxygen initially dissolved in solution (see Supporting Information for detailed analysis). Samples containing oxygen scavenging substrates were stirred and irradiated with a 450 nm CW laser in order to deoxygenate the

DOI: 10.1021/acs.inorgchem.7b01226
Inorg. Chem. 2017, 56, 9273−9280

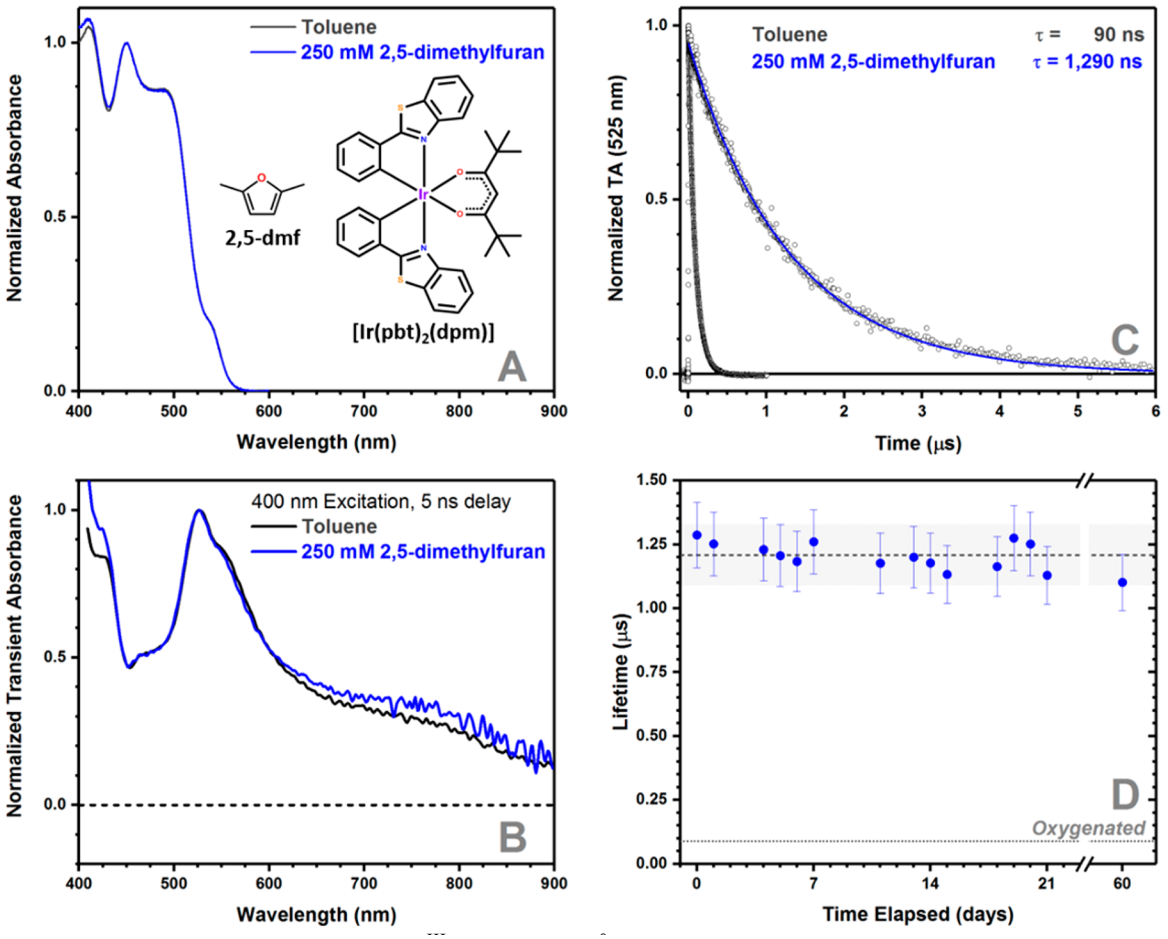

Figure 1. Photophysical data for $[Ir^{III}(pbt)_2(dpm)]^0$ in 250 mM 2,5-dimethylfuran toluene solution following irradiation at 450 nm compared to TMC-only in toluene: (A) normalized UV−vis absorbance spectra; (B) normalized transient absorbance (TA) spectra; (C) normalized TA kinetics monitored at 525 nm; (D) excited-state lifetimes monitored after sample preparation. See text for additional detail.

solution via eqs 1−4. Samples were irradiated until the maximum TMC lifetime was achieved.

Initial experiments were carried out in the nonpolar solvent toluene using the TMC $[Ir^{III}(pbt)_2(dpm)]^0$, where pbt is 2-phenylbenzothiazole and dpm is dipivaloylmethanato, with 2,5-dimethylfuran as the oxygen scavenging substrate. 2,5-Dimethylfuran was chosen because of its high solubility in common organic solvents and prior research that demonstrated rapid chemical reactivity with $^1O_2$ which results in the formation of a stable diketone product and hydrogen peroxide.[18,22]

Experimental UV−vis absorption spectra of $[Ir^{III}(pbt)_2(dpm)]^0$ in aerated toluene solutions with and without 250 mM 2,5-dimethylfuran are shown in Figure 1A. The dominant absorption bands between 400−575 nm were assigned to MLCT electronic transitions of mixed singlet and triplet character based on relatively weak extinction coefficients, $\varepsilon \approx 5000\ M^{-1}\ cm^{-1}$ (see Figure S1), and analogy to the related $[Ir^{III}(pbt)_2(acac)]^0$ compound.[23,24] Normalized TA spectra obtained 5 ns after pulsed 400 nm excitation of the $[Ir^{III}(pbt)_2(dpm)]^{0*}$ samples at room temperature are presented in Figure 1B. Excited state absorption (ESA) features were observed from 400−900 nm regardless of the presence of 2,5-dimethylfuran, and the TA spectra were superimposable for all time delays. Single wavelength kinetics were monitored at the 525 nm ESA maximum (Figure 1C) and exhibited single exponential decay behavior. The excited state lifetime of the TMC-only in toluene was 90 ns in the presence of dissolved oxygen. In contrast, $[Ir^{III}(pbt)_2(dpm)]^0$ in 250 mM 2,5-dimethylfuran toluene solution exhibited a lifetime of τ = 1.29 μs following 450 nm irradiation for 30 min.

The superimposable nature of the transient spectra and single exponential decay kinetics indicates relaxation of a single excited state back to the ground state. Additionally, a lack of chemical interaction between 2,5-dimethylfuran and $[Ir^{III}(pbt)_2(dpm)]^0$, in either the ground or excited state, is inferred from the spectrally indistinguishable UV−vis-absorption and TA spectra when comparing the TMC-only and 250 mM 2,5-dimethylfuran toluene solutions (shown in Figure S2).

The stability and longevity of the photochemically deoxygenated samples were investigated by intermittently measuring τ_{obs} over a period of several days to weeks after initial preparation. Samples were stored in the dark between measurements. Individual data points are presented with 10% error bars in Figure 1D along with the average τ_{obs} and associated 10% error (dashed line and gray shaded region, respectively). The TMC-only lifetime in toluene is represented by the dotted line for reference. Excellent long-term stability was demonstrated for the 250 mM 2,5-dimethylfuran toluene solution sample with τ_{obs} averaging 1.21 μs over measurements spanning 21 days and τ_{obs} = 1.10 μs after 60 days. In order to validate the method in polar solvents, the quintessential d^6 TMC $[Ru(bpy)_3]^{2+}$, where bpy is 2,2′-bipyridine, was chosen for use in either acetonitrile as the

DOI: 10.1021/acs.inorgchem.7b01226
Inorg. Chem. 2017, 56, 9273−9280

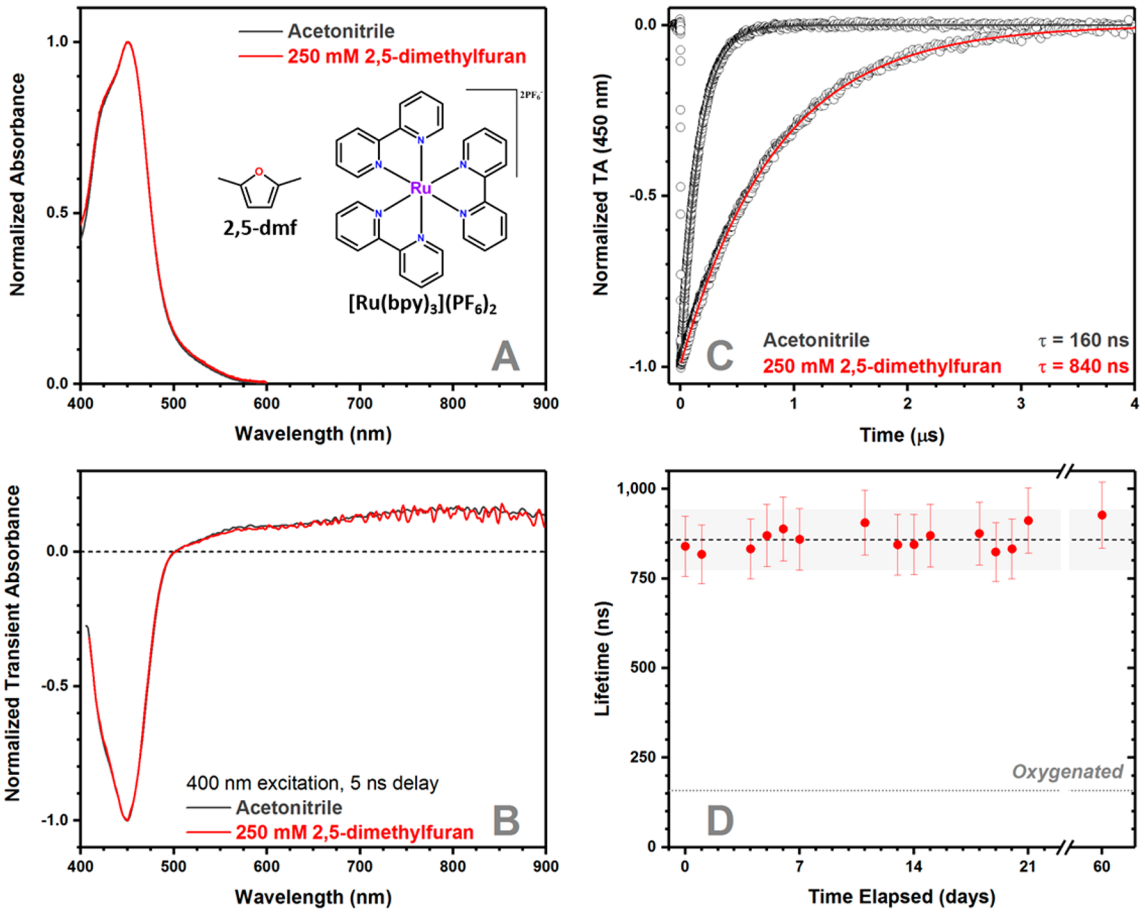

Figure 2. Photophysical data for $[Ru^{II}(bpy)_3](PF_6)_2$ in 250 mM 2,5-dimethylfuran acetonitrile solution following irradiation at 450 nm compared to TMC-only in acetonitrile: (A) normalized UV−vis absorbance spectra; (B) normalized transient absorbance (TA) spectra; (C) normalized TA kinetics monitored at 450 nm; (D) excited-state lifetimes monitored after sample preparation. See text for additional detail.

hexafluorophosphate (PF_6) salt with 2,5-dimethylfuran or aqueous solutions as the chloride salt with an amino acid due to extensive photophysical characterization of both the TMC and oxygen scavenging substrates available in the literature.[22,25,26]

UV−vis absorption spectra of the $[Ru(bpy)_3](PF_6)_2$ acetonitrile system are shown in Figure 2A. The dominant absorption bands between 400−575 nm are attributed to MLCT electronic transitions, $[Ru^{II}(bpy)_3]^{2+} \rightarrow [Ru^{III}(bpy^-)(bpy)_2]^{*2+}$.[11,25] Normalized TA spectra obtained 5 ns after pulsed 400 nm excitation of the $[Ru(bpy)_3](PF_6)_2$ samples at room temperature are presented in Figure 2B. The observed transient bleach of the MLCT band and long-wavelength ESA features were superimposable for all time delays monitored and consistent with previous results.[25] Excited state relaxation kinetics were monitored at the 450 nm bleach and well described by single exponential decay behavior with τ = 160 ns for the TMC-only solution (Figure 2C). The 2,5-dimethylfuran-containing acetonitrile sample exhibited a 5-fold enhancement of the excited state lifetime with τ = 840 ns. The photophysical characteristics of aqueous $[Ru(bpy)_3]Cl_2$ solutions containing 260 mM L-tryptophan methyl ester were identical to the $[Ru(bpy)_3](PF_6)_2$ acetonitrile solutions (Figure S3). However, the excited state lifetimes differed for the aqueous samples with τ = 370 ns for the TMC-only sample which increased to 630 ns for the 260 mM L-tryptophan methyl ester sample after irradiation. Analogous to the iridium system, no spectroscopic evidence of chemical interaction between $[Ru(bpy)_3]^{2+}$ and the oxygen scavenging substrates was observed, and the samples were stable over periods of days to weeks following the initial sample irradiation.

It is worthwhile to note that the excited-state lifetimes of argon sparged samples, which were sealed with rubber septa as opposed to PTFE stoppers, decreased to the aerated, TMC-only value after a single day of storage.

While the above measurements were performed in 2.0 mm cuvettes using a TA geometry in which the pump and probe beams were separated by a small angle, the versatility of this method was confirmed and expanded using standard 1.0 cm cuvettes in a T-shaped photoluminescence setup. This instrumental arrangement allowed for variation of the irradiation source between a 450 W Xe arc lamp and a Q-switched Nd:YAG laser equipped with an OPO tuned to 450 nm (6.6−8.8 mJ/cm^2 per pulse) while permitting the convenient collection of lifetime data. Furthermore, the method was verified to work for samples with ground state absorption values pertinent for both luminescence (A_{450nm} = 0.2) and pulsed laser (A_{450nm} = 0.6) measurements.

For the 1.0 cm cuvette measurements, the TMC samples were prepared as before with small magnetic stir bars, minimized headspace, and PTFE screw caps to seal the cells. The stirred sample solutions were irradiated for a period of time (30−60s of 10 Hz laser pulses or CW arc lamp photolysis, depending on the sample) followed by measurement of the luminescence lifetime. This process was continued until a constant τ_{obs} was reached. These experiments were conducted at high and low TMC

DOI: 10.1021/acs.inorgchem.7b01226
Inorg. Chem. 2017, 56, 9273−9280

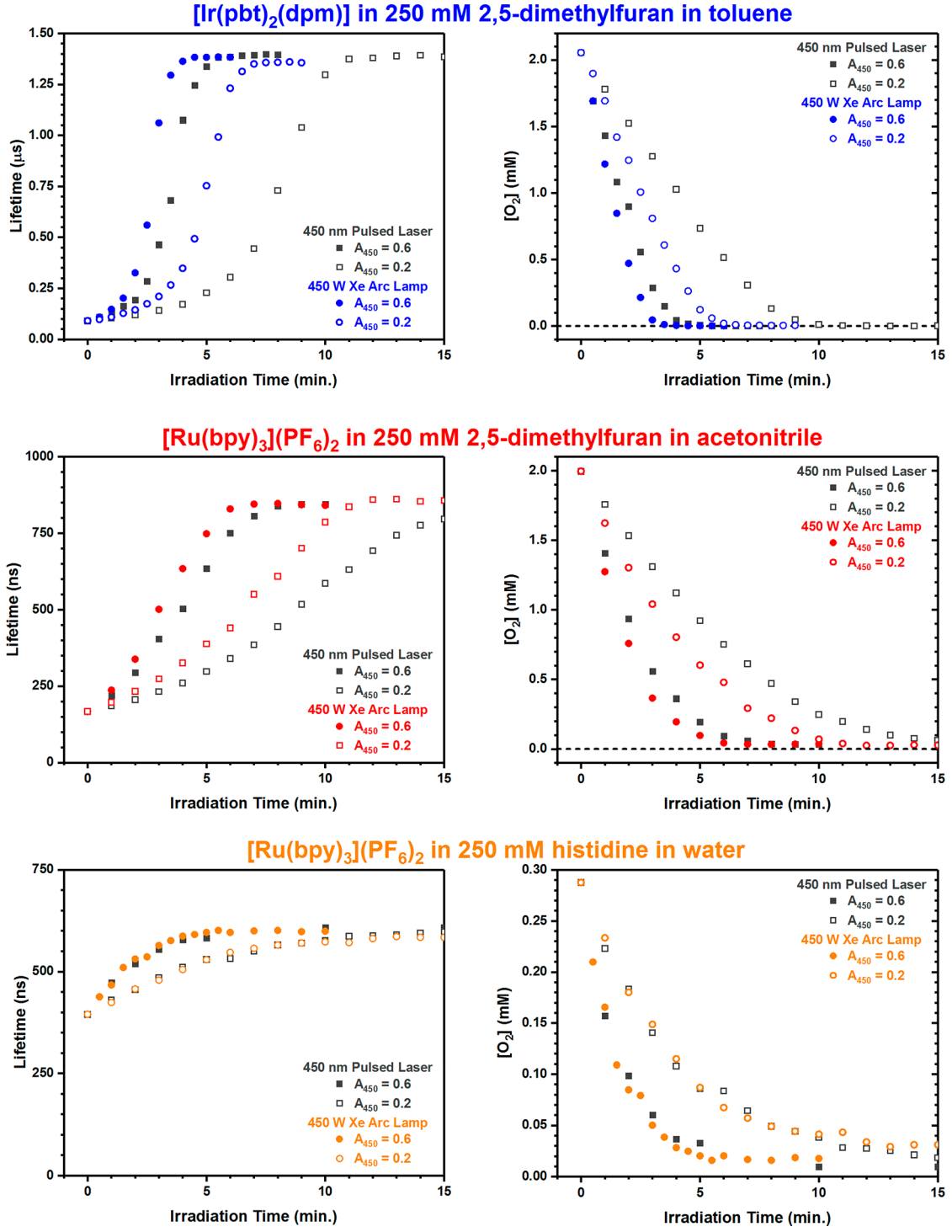

Figure 3. Excited state lifetime (left column) or dissolved oxygen concentration (right column) measured as a function of irradiation time for the TMC/scavenger/solvent combinations studied. The irradiation source used was either a 450 W Xe arc lamp (colored symbols) or pulsed 532 nm laser light (dark gray symbols). The sample absorbance at 450 nm was either 0.2 (open symbols) or 0.6 (filled symbols) in 1 cm path length cuvettes.

concentrations using both the arc lamp and laser irradiation sources for $[Ir^{III}(pbt)_2(dpm)]^0$ in 250 mM 2,5-dimethylfuran toluene solution; $[Ru(bpy)_3](PF_6)_2$ in 250 mM 2,5-dimethylfuran acetonitrile solution; and $[Ru(bpy)_3]Cl_2$ in 250 mM aqueous L-histidine. Kinetic data plots shown in terms of both luminescence lifetime or dissolved oxygen concentration as a function of irradiation time are presented for all of the combinations studied in Figure 3.

The collisional, energy transfer quenching of molecular excited states is governed by the Stern–Volmer relationship (eq 5).[26−28]

$$\frac{I_0}{I} = \frac{\tau_0}{\tau} = 1 + k_q\tau_0[Q] = 1 + K_{SV}[Q] \quad (5)$$

The fraction of excited states quenched is related to the lifetime of the chromophore in the absence of quencher (τ_0), the quencher concentration in solution ([Q]), and the bimolecular quenching rate constant (k_q). The Stern–Volmer constant, K_{SV},

DOI: 10.1021/acs.inorgchem.7b01226
Inorg. Chem. 2017, 56, 9273−9280

Table 1. Summary of Photochemical Deoxygenation Parameters for TMC/O_2 Scavenger Systems

sample	solvent	absorption (450 nm)	irradiation source	maximum lifetime (ns)	time to max lifetime (min)	$[O_2]$ at max lifetime (μM)
$[Ru(bpy)_3](PF_6)_2$ + histidine	water	0.2	lamp	590	13	29
	k_q (O_2) = 3.2 × 10^9 M^{-1} s^{-1}	0.2	laser	590	20	17
		0.6	lamp	600	5.5	16
		0.6	laser	610	10	10
		Aerated Lifetime		400		290[b]
		Freeze−Pump−Thaw Lifetime		620		0.5[c]
$[Ru(bpy)_3](PF_6)_2$ + 2,5-dimethylfuran	acetonitrile	0.2	lamp	860	12	26
	k_q (O_2) = 2.4 × 10^9 M^{-1} s^{-1}	0.2	laser	820	17	50
		0.6	lamp	850	7	34
		0.6	laser	840	9	35
		Aerated Lifetime		170		2000[b]
		Freeze−Pump−Thaw Lifetime		910		0.5[c]
$[Ir(pbt)_2(dpm)]$ + 2,5-dimethylfuran	toluene	0.2	lamp	1360	7.5	5
	k_q (O_2) = 5.0 × 10^9 M^{-1} s^{-1}	0.2	laser	1390	13	1
		0.6	lamp	1380	4.5	2
		0.6	laser	1390	6.5	1
		Aerated Lifetime		90		2050[b]
		Freeze−Pump−Thaw Lifetime		1400		0.1[c]

[a]Lifetimes given with ±10% error. [b]Determined using K_{SV} and lifetime data and in agreement with literature values in *Handbook of Photochemistry*, 3rd ed., 2006. [c]Estimated using a value of τ_0/τ = 1.001 and the respective K_{SV} for the specific chromophore and $^3O_2$.

is the product of k_q and τ_0. The lifetime of the TMC and the bimolecular quenching constant of a TMC by ground state oxygen can be independently measured. Therefore, the solution oxygen concentration, i.e. [Q], can be determined after any duration of photolysis using eq 5.

The rate of oxygen removal from the system is dependent on the quantum yield of $^1O_2$ production (eq 3) for a particular chromophore/solvent combination and the bimolecular reaction of $^1O_2$ with the scavenger molecule in solution (eq 4). The secondary, bimolecular reaction occurs under pseudo-first-order conditions ([scavenger] ≫ $[O_2]$) and will be constant throughout the photolysis. The quantum yield of $^1O_2$ production will vary depending on the concentration and lifetime of the chromophore excited-state and the $^3O_2$ concentration in solution. Explicit quantum yield values for oxygen removal were not determined for any of the chromophore solvent combinations tested because this value will change as the oxygen concentration in solution changes and detailed actinometry experiments were not performed. It is clear from the data that quantum yield values for oxygen removal vary across the chromophore/solvent systems tested. $[Ir^{III}(pbt)_2(dpm)]^0$ has the longest lifetime and was tested in toluene (2.1 mM $[^3O_2]$), resulting in the fastest rate of oxygen removal. An increase in the number of photons absorbed by or delivered to the system will result in an increase in the TMC excited-state concentration. This leads to an increase in the amount of $^1O_2$ produced, resulting in a faster rate of oxygen removal. Accordingly, an increase in the absorbance of the sample will result in a proportional increase in the rate of the chemical capture reaction. In these examples, the samples with A_{450nm} = 0.6 absorb double the number of photons as the samples with A_{450nm} = 0.2. Across the series of experiments, samples with A_{450nm} = 0.6 reach their maximum lifetime values ∼2× faster than the less absorptive samples where A_{450nm} = 0.2. Similarly, an increase in the source intensity increases the TMC excited-state concentration and the resulting oxygen capture rate. Empirically, the 450 W Xe arc lamp provides a greater photon flux than the pulsed Nd:YAG/OPO source, although detailed actinometry experiments were not conducted on either irradiation source. Additionally, the rate of oxygen removal necessarily decreases as the dissolved oxygen concentration in solution diminishes. For all data sets, an initial, rapid decrease in the ground state oxygen concentration in solution is observed (see Figure 3). The rate of the chemical capture process starts to diminish appreciably when the Stern−Volmer quenching ratio (τ_0/τ) approaches 1.10 which is the point when only 10% of excited states are quenched and when the intrinsic lifetime of the chromophore becomes the dominant relaxation pathway of the excited state. Further photolysis results in continued oxygen consumption until a plateau is reached when the Stern−Volmer quenching ratio reaches: 1.01−1.03 (1−3% excited states quenched) for $[Ir^{III}(pbt)_2(dpm)]^0$ and 250 mM 2,5-dimethylfuran in toluene; 1.05−1.10 (5−10% excited states quenched) for $[Ru(bpy)_3](PF_6)_2$ and 250 mM 2,5-dimethylfuran in acetonitrile; or 1.01−1.05 (1−5% excited states quenched) for $[Ru(bpy)_3]Cl_2$ and 250 mM L-histidine in water. In the scope of this work, we chose the irradiation time required to reach the maximum lifetime value as a simple, semiquantitative metric for sample deoxygenation. These irradiation times are provided in Table 1 for the different TMC/scavenger/solvent systems along with lifetime values obtained for aerated and freeze−pump−thaw degassed solutions for comparison.

In order to achieve the freeze−pump−thaw lifetime for any of the TMC/scavenger/solvent combinations tested, the dissolved oxygen concentration would have to decrease below 1 μM in solution. Although this method was unable to reach the 1 μM threshold, dissolved $[O_2]$ < 50 μM was consistently realized, which yielded TMC lifetimes within 10% of the freeze−pump−thaw values. The results for $[Ir^{III}(pbt)_2(dpm)]^0$ with 2,5-dimethylfuran in toluene and $[Ru(bpy)_3]Cl_2$ with L-histidine in water are particularly remarkable, as the lifetime values following

DOI: 10.1021/acs.inorgchem.7b01226
Inorg. Chem. 2017, 56, 9273−9280

irradiation are all within 5% of the freeze−pump−thaw lifetime. *Not only does this chemical capture method achieve low concentrations of dissolved oxygen, it does so in rapid fashion.* Suitable oxygen removal using traditional methods require 10−15 min of inert gas sparging or 30−60 min of freeze−pump−thaw degas cycles. This chemical capture method achieves acceptable levels of oxygen removal within this time frame, and, in some instances, achieves the requisite oxygen concentration levels of less than 50 μM in under 10 min. Along with clear applicability as a photochemical deoxygenation method for spectroscopy, this method could also prove useful for any application requiring low dissolved oxygen concentration in solution such as synthetic organic chemistry.

CONCLUSION

In summary, a method for the rapid, in situ deoxygenation of aqueous and organic solutions was demonstrated using visible light irradiation of TMCs in the presence of oxygen scavenging substrates, namely, 2,5-dimethylfuran, L-tryptophan methyl ester, and L-histidine. Enhanced excited state lifetimes, comparable with those obtained via inert gas sparging and freeze−pump−thaw techniques, were observed for sealed samples over the duration of several days to months. This method should be compatible with other known oxygen scavengers such as butylated hydroxytoluene (BHT) in organic solvents or the amino acid methionine in water. Furthermore, a plethora of TMCs and organic chromophores capable of sensitizing $^1O_2$ should behave similarly to the exemplars described herein. By employing inexpensive substrates and low-power laser light, this method provides a portable, cost-effective alternative to traditional inert gas sparging and freeze−pump−thaw degassing techniques for solution deoxygenation.

ASSOCIATED CONTENT

Supporting Information

The Supporting Information is available free of charge on the ACS Publications website at DOI: 10.1021/acs.inorgchem.7b01226.

Bulk prices of additives; ^{1}H NMR spectrum of $[Ir^{III}(pbt)_2(dpm)]^0$; analysis of O_2 headspace content; molar absorption spectrum of $[Ir^{III}(pbt)_2(dpm)]^0$; UV−visible absorption spectra for samples before and after laser irradiation; photophysical data for $[Ru(bpy)_3]Cl_2$ in 260 mM L-tryptophan methyl ester aqueous solution (PDF)

AUTHOR INFORMATION

Corresponding Authors

*(R.M.O.) E-mail: ryan.m.odonnell12.civ@mail.mil.
*(T.A.G.) E-mail: tod.grusenmeyer.ctr@us.af.mil.

ORCID

Ryan M. O'Donnell: 0000-0002-3565-9783

Funding

R.M.O., T.R.E., W.M.S., and J.S. received Army funding support provided by the ARL/SEDD Directorate, US Army Research Laboratory. T.A.G., D.J.S., and J.E.H. received Air Force funding support provided by AFRL/AFOSR and AFRL/RX Directorates, US Air Force Research Laboratory.

Notes

The authors declare no competing financial interest.

ACKNOWLEDGMENTS

This research was performed while T.A.G. held a NRC Research Associateship award at AFRL. Dr. Yiu-fai Lam and Dr. Yinde Wang of the University of Maryland Analytical NMR Service and Research Center are thanked for their assistance with NMR measurements.

ABBREVIATIONS

ESA, excited state absorption; CW, continuous wave; MLCT, metal-to-ligand charge transfer; TA, transient absorption; TMC, transition metal chromophore

REFERENCES

(1) Yoon, T. P.; Ischay, M. A.; Du, J. Visible light photocatalysis as a greener approach to photochemical synthesis. *Nat. Chem.* **2010**, *2* (7), 527−532.

(2) Shaw, M. H.; Twilton, J.; MacMillan, D. W. C. Photoredox Catalysis in Organic Chemistry. *J. Org. Chem.* **2016**, *81* (16), 6898−6926.

(3) Choi, N. W.; Verbridge, S. S.; Williams, R. M.; Chen, J.; Kim, J.-Y.; Schmehl, R.; Farnum, C. E.; Zipfel, W. R.; Fischbach, C.; Stroock, A. D. Phosphorescent nanoparticles for quantitative measurements of oxygen profiles in vitro and in vivo. *Biomaterials* **2012**, *33* (9), 2710−2722.

(4) Lo, K. K.-W.; Choi, A. W.-T.; Law, W. H.-T. Applications of luminescent inorganic and organometallic transition metal complexes as biomolecular and cellular probes. *Dalton Trans.* **2012**, *41* (20), 6021−6047.

(5) Hagfeldt, A.; Boschloo, G.; Sun, L.; Kloo, L.; Pettersson, H. Dye-Sensitized Solar Cells. *Chem. Rev.* **2010**, *110* (11), 6595−6663.

(6) Ardo, S.; Meyer, G. J. Photodriven heterogeneous charge transfer with transition-metal compounds anchored to TiO_2 semiconductor surfaces. *Chem. Soc. Rev.* **2009**, *38* (1), 115−164.

(7) Ashford, D. L.; Gish, M. K.; Vannucci, A. K.; Brennaman, M. K.; Templeton, J. L.; Papanikolas, J. M.; Meyer, T. J. Molecular Chromophore−Catalyst Assemblies for Solar Fuel Applications. *Chem. Rev.* **2015**, *115* (23), 13006−13049.

(8) Knoll, J. D.; Turro, C. Control and utilization of ruthenium and rhodium metal complex excited states for photoactivated cancer therapy. *Coord. Chem. Rev.* **2015**, *282*−*283*, 110−126.

(9) Dini, D.; Calvete, M. J. F.; Hanack, M. Nonlinear Optical Materials for the Smart Filtering of Optical Radiation. *Chem. Rev.* **2016**, *116* (22), 13043−13233.

(10) Singh-Rachford, T. N.; Castellano, F. N. Photon upconversion based on sensitized triplet−triplet annihilation. *Coord. Chem. Rev.* **2010**, *254* (21−22), 2560−2573.

(11) Thompson, D. W.; Ito, A.; Meyer, T. J. $[Ru(bpy)_3]^{2+*}$ and other remarkable metal-to-ligand charge transfer (MLCT) excited states. *Pure Appl. Chem.* **2013**, *85* (7), 1257.

(12) Solvent Properties. In *Handbook of Photochemistry*, 3rd ed.; Montalti, M.; Credi, A.; Prodi, L.; Gandolfi, M. T., Eds.; CRC Press: Boca Raton, FL, 2006; pp 535−559.

(13) Schweitzer, C.; Schmidt, R. Physical Mechanisms of Generation and Deactivation of Singlet Oxygen. *Chem. Rev.* **2003**, *103* (5), 1685−1758.

(14) DeRosa, M. C.; Crutchley, R. J. Photosensitized singlet oxygen and its applications. *Coord. Chem. Rev.* **2002**, *233*−*234*, 351−371.

(15) Ashen-Garry, D.; Selke, M. Singlet Oxygen Generation by Cyclometalated Complexes and Applications. *Photochem. Photobiol.* **2014**, *90* (2), 257−274.

(16) Gao, R.; Ho, D. G.; Hernandez, B.; Selke, M.; Murphy, D.; Djurovich, P. I.; Thompson, M. E. Bis-cyclometalated Ir(III) Complexes as Efficient Singlet Oxygen Sensitizers. *J. Am. Chem. Soc.* **2002**, *124* (50), 14828−14829.

(17) Prein, M.; Adam, W. The Schenck Ene Reaction: Diastereoselective Oxyfunctionalization with Singlet Oxygen in Synthetic Applications. *Angew. Chem., Int. Ed. Engl.* **1996**, *35* (5), 477−494.

DOI: 10.1021/acs.inorgchem.7b01226
Inorg. Chem. 2017, 56, 9273−9280

(18) Mongin, C.; Golden, J. H.; Castellano, F. N. Liquid PEG Polymers Containing Antioxidants: A Versatile Platform for Studying Oxygen-Sensitive Photochemical Processes. *ACS Appl. Mater. Interfaces* **2016**, *8* (36), 24038−24048.
(19) Filatov, M. A.; Baluschev, S.; Landfester, K. Protection of densely populated excited triplet state ensembles against deactivation by molecular oxygen. *Chem. Soc. Rev.* **2016**, *45* (17), 4668−4689.
(20) Baranoff, E.; Curchod, B. F. E.; Frey, J.; Scopelliti, R.; Kessler, F.; Tavernelli, I.; Rothlisberger, U.; Grätzel, M.; Nazeeruddin, M. K. Acid-induced degradation of phosphorescent dopants for OLEDs and its application to the synthesis of tris-heteroleptic iridium(III) bis-cyclometalated complexes. *Inorg. Chem.* **2012**, *51* (1), 215−224.
(21) Frey, J.; Curchod, B. F. E.; Scopelliti, R.; Tavernelli, I.; Rothlisberger, U.; Nazeeruddin, M. K.; Baranoff, E. Structure-property relationships based on Hammett constants in cyclometalated iridium-(III) complexes: their application to the design of a fluorine-free FIrPic-like emitter. *Dalton Trans.* **2014**, *43* (15), 5667−5679.
(22) Wilkinson, F.; Helman, W. P.; Ross, A. B. Rate Constants for the Decay and Reactions of the Lowest Electronically Excited Singlet State of Molecular Oxygen in Solution. An Expanded and Revised Compilation. *J. Phys. Chem. Ref. Data* **1995**, *24* (2), 663−677.
(23) Lamansky, S.; Djurovich, P.; Murphy, D.; Abdel-Razzaq, F.; Kwong, R.; Tsyba, I.; Bortz, M.; Mui, B.; Bau, R.; Thompson, M. E. Synthesis and Characterization of Phosphorescent Cyclometalated Iridium Complexes. *Inorg. Chem.* **2001**, *40* (7), 1704−1711.
(24) Laskar, I. R.; Chen, T.-M. Tuning of Wavelengths: Synthesis and Photophysical Studies of Iridium Complexes and Their Applications in Organic Light Emitting Devices. *Chem. Mater.* **2004**, *16* (1), 111−117.
(25) Arias-Rotondo, D. M.; McCusker, J. K. The photophysics of photoredox catalysis: a roadmap for catalyst design. *Chem. Soc. Rev.* **2016**, *45* (21), 5803−5820.
(26) Feng, T.; Grusenmeyer, T. A.; Lupin, M.; Schmehl, R. H. Following Oxygen Consumption in Singlet Oxygen Reactions via Changes in Sensitizer Phosphorescence. *Photochem. Photobiol.* **2015**, *91* (3), 705−713.
(27) Balzani, V.; Ceroni, P.; Juris, A. In *Photochemistry and Photophysics: Concepts, Research, Applications*; Wiley-VCH: 2014; pp 139−169.
(28) Balzani, V.; Bolletta, F.; Scandola, F. Vertical and "nonvertical" energy transfer processes. A general classical treatment. *J. Am. Chem. Soc.* **1980**, *102* (7), 2152−2163.

DOI: 10.1021/acs.inorgchem.7b01226
Inorg. Chem. 2017, 56, 9273−9280